PNAS RESEARCH ARTICLE | MICROBIOLOGY OPEN ACCESS

Expanding the genetic toolkit helps dissect a global stress response in the early-branching species *Fusobacterium nucleatum*

Falk Ponath[a], Yan Zhu[b], Valentina Cosi[a], and Jörg Vogel[a,b,1]

Edited by Carol Gross, University of California, San Francisco, CA; received January 28, 2022; accepted August 13, 2022

***Fusobacterium nucleatum*, long known as a common oral microbe, has recently garnered attention for its ability to colonize tissues and tumors elsewhere in the human body. Clinical and epidemiological research has now firmly established *F. nucleatum* as an oncomicrobe associated with several major cancer types. However, with the current research focus on host associations, little is known about gene regulation in *F. nucleatum* itself, including global stress-response pathways that typically ensure the survival of bacteria outside their primary niche. This is due to the phylogenetic distance of Fusobacteriota to most model bacteria, their limited genetic tractability, and paucity of known gene functions. Here, we characterize a global transcriptional stress-response network governed by the extracytoplasmic function sigma factor, σ^E. To this aim, we developed several genetic tools for this anaerobic bacterium, including four different fluorescent marker proteins, inducible gene expression, scarless gene deletion, and transcriptional and translational reporter systems. Using these tools, we identified a σ^E response partly reminiscent of phylogenetically distant Proteobacteria but induced by exposure to oxygen. Although *F. nucleatum* lacks canonical RNA chaperones, such as Hfq, we uncovered conservation of the noncoding arm of the σ^E response in form of the noncoding RNA FoxI. This regulatory small RNA acts as an mRNA repressor of several membrane proteins, thereby supporting the function of σ^E. In addition to the characterization of a global stress response in *F. nucleatum*, the genetic tools developed here will enable further discoveries and dissection of regulatory networks in this early-branching bacterium.**

Fusobacterium | extracytoplasmic sigma factor | noncoding RNA | small RNA | posttranscriptional control

Significance

Fusobacterium nucleatum is an abundant member of the oral microbiome that can spread throughout the body and colonize secondary sites, including cancer tissues, where it promotes tumor progression. Understanding how *F. nucleatum* adapts to these various environments might open new therapeutic opportunities, but we currently lack basic molecular knowledge of gene regulation in this phylogenetically distinct bacterium. We developed much-needed genetic tools for use in *F. nucleatum* and with their aid uncovered a stress response mediated by the transcriptional activator σ^E and an associated small RNA. Our findings in an early-branching bacterium reveal surprising parallels to and differences from the σ^E response in well-characterized model bacteria, and provide a framework that will accelerate research into the understudied phylum Fusobacteriota.

The oral microbe *Fusobacterium nucleatum* is an abundant member of the oral microbiome, a complex microbial community consisting of over 700 species (1). In the oral cavity, *F. nucleatum* functions as a bridging organism between colonizers of dental plaque (2) and is crucial for the maintenance of this biofilm (3). While generally considered a mutualist, *F. nucleatum* is also implicated in periodontitis and occurs in abscesses in various body sites (4). Most importantly, *F. nucleatum* has recently garnered broad attention for its association with several different types of human tumors. The bacterium is highly abundant in tissues of colorectal, breast, esophageal, and pancreatic cancer (5–11), and colonization with *F. nucleatum* is associated with enhanced tumor growth, metastasis, and resistance to chemotherapy (9–11). These tissues represent new and adverse environments very different from *F. nucleatum*'s primary niche in the oral cavity.

The occurrence of *F. nucleatum* at these extraoral sites implies that this bacterium can sense and adapt to changes in its environment. To date, however, only two regulatory circuits have been described in *F. nucleatum*: the two-component systems (TCS) CarRS and ModRS, which control interspecies coaggregation and resistance to hydrogen peroxide, respectively. Both also play a role in bacterial virulence (12, 13). Factors that govern global stress responses are unknown. Decoding molecular principles of gene regulation in *F. nucleatum* has generally been difficult for two reasons. First, the phylum Fusobacteriota is phylogenetically remote from all model bacteria (14) (Fig. 1*A*), which hampers knowledge transfer by sequence comparison. Second, functional genetics in this obligate anaerobic, gram-negative bacterium is in its infancy (2), being limited to two recently introduced systems for scarless genomic deletion (15, 16) and to plasmid-based overexpression of a gene of interest (17). Therefore, new genetic tools are much needed to systematically identify and characterize regulatory pathways that ensure viability of *F. nucleatum* under stress conditions. In this work, we expand the fusobacterial genetic tool-kit and use it to dissect a global stress response composed of the extracytoplasmic function (ECF) σ factor, σ^E, and an associated regulatory small RNA (sRNA).

ECFs present a fundamental signal transduction mechanism whereby bacteria monitor their environment (18). Specifically, ECFs are usually involved in regulating the

Author affiliations: [a]Helmholtz Institute for RNA-based Infection Research (HIRI), Helmholtz Centre for Infection Research (HZI), Würzburg, D-97080 Germany; and [b]Institute for Molecular Infection Biology, University of Würzburg, Würzburg, D-97080 Germany

Author contributions: F.P. and J.V. designed research; F.P., Y.Z., and V.C. performed research; F.P. and J.V. analyzed data; and F.P. and J.V. wrote the paper.

The authors declare no competing interest.

This article is a PNAS Direct Submission.

[1]To whom correspondence may be addressed. Email: joerg.vogel@uni-wuerzburg.de.

This article contains supporting information online at http://www.pnas.org/lookup/suppl/doi:10.1073/pnas.2201460119/-/DCSupplemental.

Published September 26, 2022.

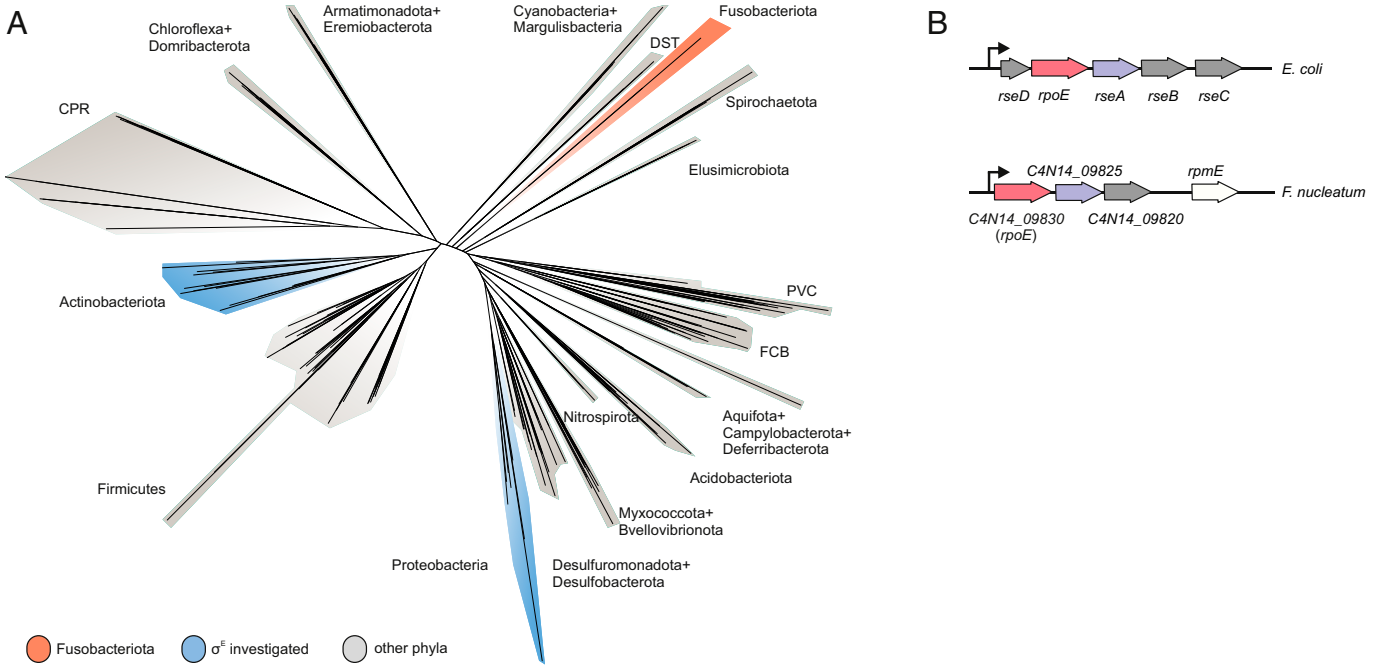

Fig. 1. Phylogenetic positioning of Fusobacteriota and comparison of the ECF locus. (*A*) A phylogenetic tree of 265 bacterial species based on the alignments provided by Coleman et al. (14). (*B*) Schematic representation of the *rpoE* operon in *E. coli* and *F. nucleatum*. *rpoE* genes are in red; the anti-σ factor *rseA* and its putative homolog in *F. nucleatum* are in purple; the remaining genes in the respective *rpoE* operons are in gray.

integrity of the bacterial envelope (19), which represent the first line of defense in gram-negative bacteria (20). ECFs across different phyla are activated by a variety of signaling stimuli, including broad stresses—such as osmotic stress, heat shock, oxidative stress (20)—but also more specific stressors, such as singlet oxygen produced by photosynthesis (21) or lysozyme (22). Nevertheless, ECFs share similar core features: 1) they are autoregulatory; 2) an anti-σ factor that keeps the ECF in an inactive state is encoded in the same operon; and 3) upon sensing of the specific signal the anti-σ factor is inactivated either through proteolytic degradation (23), conformational changes (24, 25), or sequestration by a third protein (26). More rarely, ECFs can also be activated through phosphorylation (27) or via a TCS (28).

The σ^E response has been particularly well-studied since its discovery in *Escherichia coli* more than three decades ago (29). Upon envelope stress, proteolytic cleavage and degradation of the anti-σ factor RseA releases σ^E from the inner membrane (IM) into the cytosol, where σ^E activates the transcription of >100 genes (30, 31). The σ^E regulon is functionally similar across different bacterial species and includes genes involved in DNA damage repair, liposaccharide biogenesis, and outer membrane (OM) homeostasis (31–35).

Importantly, the σ^E regulon also includes several sRNAs genes, which together constitute the "noncoding arm" of the response (36). Work in *E. coli*, *Salmonella*, and *Vibrio* species has established that these σ^E-controlled sRNAs posttranscriptionally repress mRNAs of diverse envelope proteins, including many major OM proteins (OMPs) (37–45). Endowing the transcriptional activator σ^E with a repressor function, these sRNAs act synergistically to ensure envelope integrity. In all species investigated thus far, these sRNAs work in conjunction with the general RNA chaperone Hfq, which aids base pairing between the sRNAs and their target mRNAs. In fact, chronic activation of the σ^E response as a result of perturbed envelope homeostasis is a conserved characteristic of *hfq* deletion strains among these species (46–49).

The envelope composition of *F. nucleatum* is largely unknown, and there has been conflicting evidence with respect to a potential σ^E stress response. First, genome annotation of *F. nucleatum* (50) predicted a putative *rpoE* gene, which encodes σ^E in *E. coli* (Fig. 1*B*). However, a recent comprehensive phylogenetic analysis placed the putative *F. nucleatum* σ^E in a functionally different ECF group from the *E. coli* protein (51). Second, our recent RNA-sequencing (RNA-seq) study in *F. nucleatum* discovered a previously unknown large suite of sRNAs. Preliminary analysis identified one of these sRNAs, FoxI, as a posttranscriptional repressor of an abundant OMP (17). However, FoxI was induced by molecular oxygen, a condition which seems unrelated to envelope stress and untypical of a σ^E response. More importantly, *F. nucleatum* lacks a gene coding for Hfq or any other known sRNA chaperone.

Here, to experimentally resolve these seeming inconsistencies, we developed several much-needed systems to characterize fusobacterial gene regulation: fluorescent marker proteins, transcriptional and translational reporters, an inducible gene-expression system, and a gene-deletion system that is not reliant on a specific strain background. Application of these tools allowed us to define the σ^E regulon of *F. nucleatum*, revealing a surprising conservation of its overall architecture in this early-branching species. This general conservation includes a noncoding arm of the σ^E response provided by the sRNA FoxI, which we show acts as a negative posttranscriptional regulator of several envelope proteins. Intriguingly, the fusobacterial ECF is activated by oxygen rather than sources of envelope or oxidative stress. Our results provide functional evidence for a global stress response composed of a σ factor and an associated sRNA in an early-branching bacterium, and an experimental framework to dissect regulatory networks in the understudied phylum Fusobacteriota.

Results

Expanding the Genetic Toolkit for *F. nucleatum*. To facilitate dissection of gene regulatory networks in *F. nucleatum*, we created

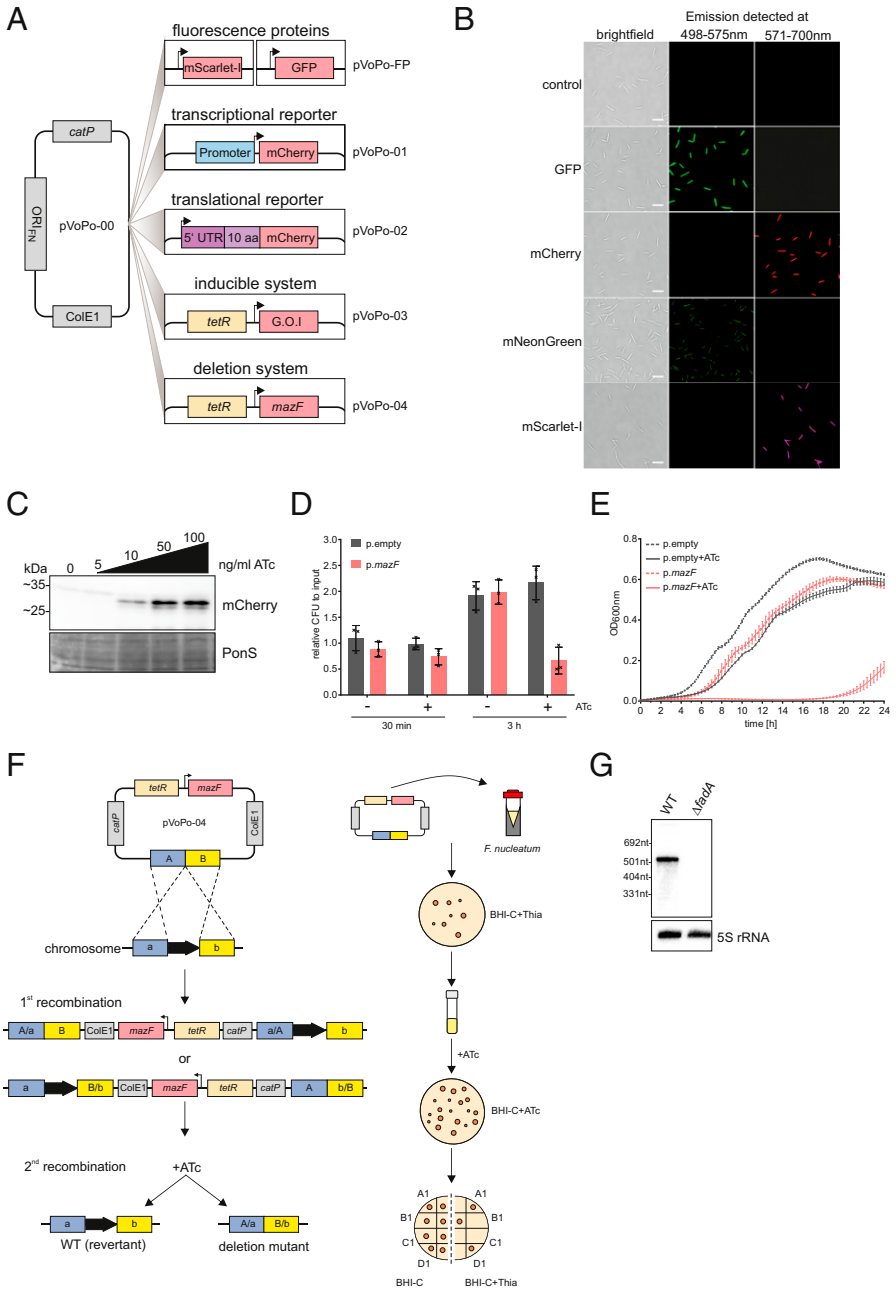

Fig. 2. A genetic toolbox for *F. nucleatum*. (*A*) Overview of the plasmid-based genetic tools developed for *F. nucleatum* based on the vector pVoPo-00. *catP*, chloramphenicol resistance cassette; ColE1, replication of origin; FP, fluorescent protein (GFP, mCherry, mNeonGreen, mScarlet-I); G.O.I, gene of interest; ORI_{FN}, origin of replication for *F. nucleatum*; *tetR*, tetracycline repressor. (*B*) Representative images of *F. nucleatum* carrying pVoPo-FP expressing different fluorescent proteins. The cells were PFA-fixated prior to overnight maturation at 4 °C. The emission was detected at the indicated wavelength. (Scale bars, 5 μm.) (*C*) Western blot analysis of lysates of *F. nucleatum* carrying a plasmid with *mCherry* introduced in the inducible system (pVoPo-03) after 30-min exposure to different ATc concentrations. mCherry runs as a duplet likely representing the full-length protein as well as a truncated version arising from an internal translational start site (53). Ponceau S (PonS) staining is shown as loading control. (*D*) Quantification of colony-forming units (CFU) for *F. nucleatum* carrying the empty vector control pVoPo-03 (p.empty) or the pVoPo-03-*mazF* plasmid (p.*mazF*). The bacteria were grown to mid-exponential phase and treated with 100 ng mL^{-1} ATc to induce *mazF* expression. Serial dilutions of the samples were plated after 0 min (input), 30 min, and 3 h. Untreated samples were used as control. Data are presented as the average and SD for three biological replicates relative to the input CFUs. (*E*) Growth curves for *F. nucleatum* carrying either p.empty or p.*mazF* in the presence or absence of 100 ng mL^{-1} ATc. No selection pressure for plasmid maintenance was included. Displayed is the average of three biological replicates with SD. (*F*) Schematic representation of allelic exchange (*Left*) and experimental workflow (*Right*) using the pVoPo-04 system to generate unmarked deletion strains. A/B, up- and downstream homology regions. (*G*) Northern blot detection of *fadA* using total RNA samples extracted from *F. nucleatum* WT or a Δ*fadA* strain generated via the deletion system pVoPo-04. 5S rRNA served as loading control.

five plasmid-based tools: constitutively expressed fluorescent marker proteins, a transcriptional and a translational reporter system, an inducible gene expression system, and a system for markerless genomic deletion (Fig. 2*A*). These systems are derived from our recently developed plasmid pEcoFus for gene overexpression in *F. nucleatum* (17). We initially reduced the overall size of pEcoFus, generating the plasmid pVoPo-00 (see *Materials and Methods* for details). Next, we inserted an expression cassette for one of four different codon-optimized fluorescent proteins: mCherry, GFP, mScarlet-I, and mNeonGreen. These constructs allow easy visualization of *F. nucleatum* using fluorescence imaging (Fig. 2*B*). pVoPo-mNeonGreen uses an expression construct with a weaker promoter, therefore the fluorescence signal is lower (*Materials and Methods*). This adjustment was necessary because

we were unable to express the original mNeonGreen construct in *E. coli* during the cloning procedure, likely due to overexpression toxicity. The pVoPo-mNeonGreen construct also demonstrates that marker gene expression can be adjusted and thereby adapted to the conditions needed. In addition to their excitation and emission spectra, the four fluorescent proteins also differ in photostability and maturation time. This will allow researchers to choose the optimal vector for their specific experimental needs.

On the basis of pVoPo-mCherry, we generated the transcriptional reporter plasmid pVoPo-01 to determine the activity of promoter regions of interest placed upstream of mCherry (Fig. 2*A*). For translational reporters (plasmid pVoPo-02), the 5′ UTR and first 10 aa of a specific target gene are fused to the second codon of mCherry and expressed from a constitutive promoter (Fig. 2*A*).

Next, we adapted the widely used tetracycline-inducible gene-expression system (52) for use in *F. nucleatum*. To this end, we replaced the constitutive promoter of pVoPo-00 with a synthetic tetracycline-responsive promoter and added a TetR repressor gene, thus creating plasmid pVoPo-03. For proof of concept, we showed that expression of mCherry from this plasmid can be tightly controlled with the nonbacteriostatic tetracycline derivative, anhydrotetracycline (ATc). Addition of different concentrations of ATc to cultures of *F. nucleatum* led to a dose-dependent and robust expression of mCherry (Fig. 2*C*), whereas no signal was detected in the absence of ATc. Of note, in the western blots, mCherry runs as a doublet, likely representing full-length protein and a truncated version expressed from an internal translational start site (53).

Gene deletion represents another important tool in the arsenal to study gene regulation in bacteria. The currently available gene disruption (54, 55) and deletion (15,16) tools for *F. nucleatum* use suicide vectors. However, these vectors require either constant selection pressure (56, 57) or a *galK(T)* gene-deletion background for efficient counterselection (15, 16), which limits their application for long-term or complex experiments, such as animal studies. Taking advantage of the inducible plasmid pVoPo-03, we evaluated the MazF toxin as a potential counterselection marker, since heterologous expression of this endonuclease had been shown to be toxic in several unrelated bacteria (58–60). Similarly, in *F. nucleatum* we observed a 40% reduction in viable bacteria 3 h after *mazF* induction (Fig. 2*D*). Induced expression of MazF caused a drastic growth delay for ∼16 h, before growth resumed (Fig. 2*E*). Importantly, no recovery was observed when this experiment was performed under conditions that select for plasmid retention (*SI Appendix*, Fig. S1). Therefore, only bacteria that have lost the plasmid will grow. These observations indicated the feasibility of using inducible *mazF* expression as a method for counterselection during double cross-over homologous recombination, as depicted in Fig. 2*F*. We successfully validated this approach by deleting the adhesin gene *fadA* in *F. nucleatum*, as evident from the absence of *fadA* mRNA on a northern blot (Fig. 2*G*). In combination, these five plasmid-based systems developed here provide much-needed genetic tools to accelerate functional genomics in *F. nucleatum* and likely other members of the understudied phylum of Fusobacteriota.

The σ^E Regulon in *F. nucleatum*. To define a potential σ^E stress response in *F. nucleatum*, we cloned the candidate fusobacterial *rpoE* gene C4N14_09830 into the inducible pVoPo-03 plasmid. We then used RNA-seq to determine the initial transcriptional response upon induction of this gene for 30 min during mid-exponential growth. Expression of C4N14_09830 did not affect bacterial growth at this time point (*SI Appendix*, Fig. S2); in fact, growth inhibition was observed only 2.5 h after induction. This indicates that aberrant activation of C4N14_09830 negatively affects cell growth only upon prolonged expression. Applying a false-discovery rate (FDR) of ≤ 0.05, our global gene-expression analysis identified 147 up-regulated ($\log_2$ fold-change ≥ 1) and 23 down-regulated ($\log_2$ fold-change ≤ -1) genes, as compared to empty vector control (Fig. 3*A*). The down-regulated transcripts mostly encode membrane proteins and include an ortholog of the IM galactose transporter MglB and three similar multicistronic operons encoding envelope proteins, such as a FadA-domain containing protein, OmpA family proteins and type 5a autotransporters (Dataset S1).

Analysis of the promoter regions of the up-regulated genes revealed a common motif with a "GTCWAA" in the −10 box and a less distinct "AAC" in the −35 box separated by an AT-rich spacer region (Fig. 3*B*). This motif closely resembles the well-established consensus σ^E binding sites in *E. coli* or *Pseudomonas aeruginosa* (61, 62). Additionally, the 18-nt spacing between the transcriptional start site (TSS) and the −10 box is very similar to *E. coli* (*SI Appendix*, Fig. S3) (31). Importantly, this motif is distinct from the previously identified σ^{70} binding site, in both the −10 and −35 regions (Fig. 3*B*). The putative σ^E motif is present in 28 transcriptional units consisting of 127 genes and accounted for 113 of the 144 up-regulated genes (Dataset S1). Interestingly, we observed that in 14 cases σ^E activation initiated transcription of suboperons (Dataset S1), leading to an uncoupling of gene expression from the upstream genes of these operons.

Besides the candidate *rpoE* gene itself, the two downstream genes in its operon (Fig. 1*B*) were also highly up-regulated upon induction of this putative ECF (Fig. 3*A*), reflecting the established self-amplification of the σ^E response in *E. coli*, where σ^E directly activates its own promoter (63).

Despite the evolutionary distance of Fusobacteriota to Proteobacteria (Fig. 1*A*) (14), the transcriptional response described here exhibits several similar features to the σ^E regulon in *E. coli*. This includes, for example, up-regulation of homologous genes important for the insertion of OMPs (*bamA*, *skp*) or lipid A biosynthesis (*lxpD*) (31, 33, 64–66). The observed target gene conservation classifies the candidate ECF protein C4N14_09830 as a σ^E homolog and thus we will refer to it as σ^E from here on. Interestingly, three genes (*ftsY*, *secA*, *lepB*) essential for Sec-dependent (general secretory pathway-dependent) protein translocation across the IM (67, 68) were induced as well; none of them had previously been linked to σ^E. Twenty-four genes in the transcriptional response lack any functional prediction, including the most highly up-regulated dicistronic operon C4N14_03280-C4N14_03285 (Fig. 3*A*). This raises the question of whether these genes are involved in envelope maintenance or protein translocation as well, or if they represent an entirely new function in the σ^E-mediated stress response.

Recent studies have identified σ^E-activated sRNAs in several different species (39–42, 49, 69, 70). Here, we observed a clear increase of the levels the oxygen-induced 87-nt sRNA FoxI upon induced expression of σ^E in *F. nucleatum* (17). This regulation suggests that the fusobacterial σ^E response might possess a noncoding arm, to which we will return below.

Validation of σ^E Target Genes Using Transcriptional Reporters. To confirm a subset of the identified σ^E target genes with an orthogonal method, we constructed five transcriptional reporters, in which the promoter regions of these targets, including the sRNA FoxI, drive mCherry expression. To confirm that the fusobacterial σ^E protein controls its own transcription, we included

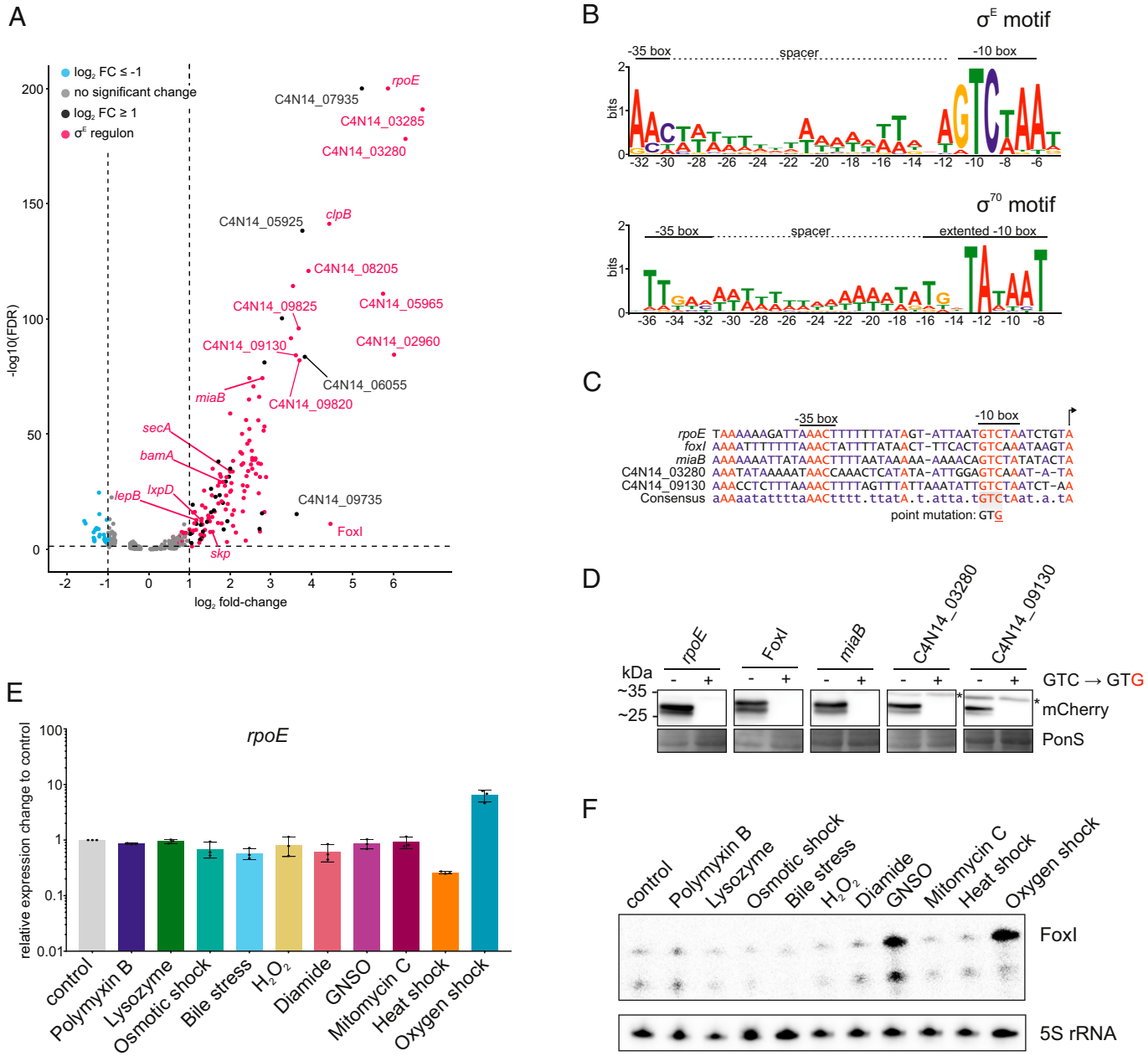

Fig. 3. The σ^E regulon in *F. nucleatum*. (*A*) Volcano plot of the global gene-expression changes in *F. nucleatum* after 30 min of σ^E induction. Gene expression of bacteria carrying pVoPo-03-σ^E is compared to cells carrying pVoPo-03 serving as empty vector control. Genes were considered significantly up-regulated with a $\log_2$ fold-change ≥ 1 (black) and significantly down-regulated with a $\log_2$ fold-change ≤ −1 (blue) with an FDR ≤ 0.05 (dashed horizontal line). The σ^E regulon (red) includes all transcriptional units that harbor the identified σ^E binding motif in their promoter region. (*B, Upper*) motif analysis via MEME (102) for all genes significantly up-regulated upon σ^E induction. TSS of all up-regulated genes were manually annotated and 50 nt upstream of the identified TSSs were used as input for MEME. The conserved −10 and −35 boxes are indicated, as well as the AT-rich spacer in between both boxes. (*Lower*) The previously identified promoter motif for σ^{70} with an extended −10 box and a less pronounced −35 box (17). (*C*) Alignment of the promoter regions for selected genes identified as part of the σ^E regulon. A point mutation inserted into transcriptional reporter constructs (see *D*) is indicated. (*D*) Western blot analysis for mCherry expressed from transcriptional reporter plasmids harboring the native promoters (GTC) or a point mutation in the conserved −10 box (GTG) for selected genes shown in *C*. Total proteins samples were collected during mid-exponential phase for western blot analysis. PonS staining is shown as loading control. Representative images of three independent experiments are shown. Unspecific bands are marked by an asterisk. (*E*) qRT-PCR analysis for *rpoE* mRNA after exposing *F. nucleatum* to the indicated stress conditions for 60 min. Data are normalized to the control and plotted as the average of three biological replicates with the SD. (*F*) Northern blot probed for the sRNA FoxI using total RNA samples extracted from *F. nucleatum* treated with the indicated stress conditions for 60 min. The smaller band represents a degradation or degradation event.

the promoter of the *rpoE* gene. All these promoters harbor in their −10 region a conserved cytosine shown to be critical for recognition by σ^E in *E. coli* (71) (Fig. 3*C*). Strikingly, a C-to-G point mutation at this position completely abolished transcription from these five selected fusobacterial promoters (Fig. 3*D*). These data indicate that these genes depend on σ^E for their transcriptional activation and support the relevance of the identified promoter motif for recognition by σ^E.

Oxygen-Dependent Activation of the σ^E Response in *F. nucleatum*. It is well established that σ^E is activated in different bacterial species by various distinct stressors, such as unfolded proteins, osmotic stress, heat shock, singlet oxygen, or oxidative stress (20,21,29,72,73). To better understand what activates σ^E in *F. nucleatum*, we monitored *rpoE* mRNA levels upon exposure to different sources of envelope (polymyxin B; lysozyme; bile), osmotic (NaCl), and oxidative stress (H_2O_2; diamide;

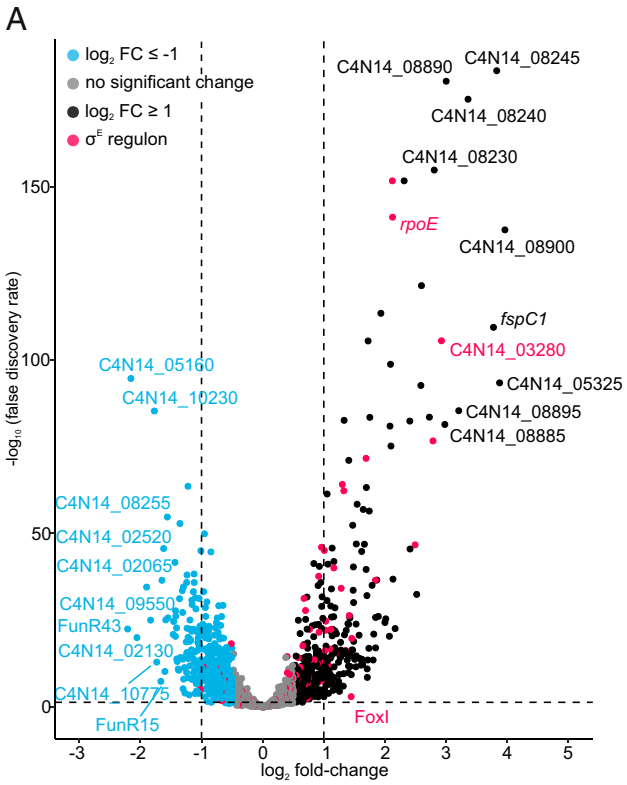

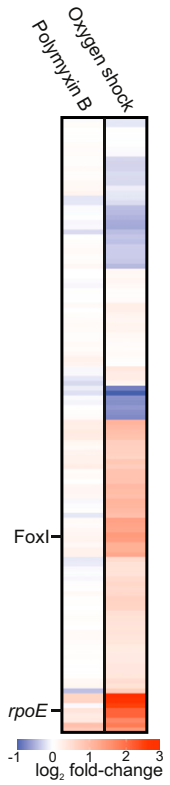

Fig. 4. Transcriptional response of the anaerobe *F. nucleatum* to oxygen. (*A*) Volcano plot of the global gene-expression changes in *F. nucleatum* after 20 min of oxygen exposure. Differential expression analysis was carried out by comparing the treated samples to an untreated control kept in the anaerobic chamber. Genes were considered significantly up-regulated with a $\log_2$ fold-change ≥ 1 (black) and significantly down-regulated with a $\log_2$ fold-change ≤ -1 (blue) with an FDR ≤ 0.05 (dashed horizontal line). The σ^E regulon (red) contains all transcriptional units that harbor the identified binding motif in their promoter region. (*B*) Overview of the gene-expression changes for all members of the σ^E regulon upon exposure to 400 ng mL^{-1} polymyxin B or oxygen exposure for 20 min. The heatmap displays the $\log_2$ fold-changes. The sRNA FoxI and *rpoE* are indicated.

S-nitrosoglutathione [GNSO]); DNA damage (mitomycin C), heat shock (42 °C), and oxygen exposure (Fig. 3*E*). Surprisingly, in this anaerobe bacterium, we observed a selective σ^E induction upon oxygen exposure. Importantly, the envelope-penetrating antibiotic polymyxin B, which is a well-established activator of σ^E in *E. coli*, did not induce *rpoE* in *F. nucleatum*, despite the fact that polymyxin B is active against this gram-negative species (74).

FoxI, originally reported as an oxygen-responsive sRNA, is now found to possess a promoter that is stringently controlled by σ^E (Fig. 3 *C* and *D*). Profiling FoxI expression in response to the full panel of stressors described above, we observed an almost selective increase in FoxI levels upon oxygen exposure (Fig. 3*F* and *SI Appendix*, Fig. S4), with the exception of nitrosative oxidative stress (GNSO) that induced this sRNA as well. Interestingly, *rpoE* mRNA levels did not increase after treatment with GNSO, suggesting that σ^E might not be the only regulator of FoxI (Fig. 3 *E* and *F*). Supporting the strong induction of σ^E upon oxygen exposure, the transcripts of four additional genes of the σ^E regulon showed a similar increase after oxygen exposure in comparison to the untreated control (*SI Appendix*, Fig. S5).

F. nucleatum subspecies *nucleatum*, used in this study, harbors no additional ECFs. Yet, it does encode three conserved σ factors (*SI Appendix*, Fig. S6*A*): housekeeping RpoD, a second uncategorized σ^{70}-family member C4N14_05515, and a putative homolog of SigH of the Clostridiales. The strain we used also harbors a rare putative σ factor (C4N14_03400) found only in some members of Fusobacterales, Staphylococci, Clostridiaceae, and on plasmids of Enterococcaceae. The alternative σ factor RpoN is absent in the *F. nucleatum* subspecies *nucleatum* strain used here. Testing a possible activation of the three conserved σ factors under different stress conditions by using qRT-PCR, we observed only mild expression changes upon oxygen exposure (*SI Appendix*, Fig. S6*B*). According to our RNA-seq data, these σ factor genes do not respond to σ^E either (Dataset S1), suggesting that σ^E is a main factor in the response to molecular oxygen.

Global Analysis of the Oxygen Response in *F. nucleatum*. In light of the specific activation of σ^E and FoxI by oxygen (Fig. 3 *E* and *F*), we investigated the global activation of the σ^E regulon by exposing *F. nucleatum* to oxygen for 20 min, followed by RNA-seq analysis. We observed a total of 289 significantly regulated genes (FDR ≤ 0.05) with 174 up-regulated ($\log_2$ fold-change ≥ 1) and 115 down-regulated genes ($\log_2$ fold-change ≤ -1) (Fig. 4*A*). The upregulated genes included the *rpoE* operon and the sRNA FoxI confirming their activation by oxygen. Nineteen additional genes of the σ^E regulon identified in Fig. 3*A* were also up-regulated (Fig. 4*B*), including the dicistronic operon C4N14_03280-C4N14_03285. Of note, sensing of oxygen by *F. nucleatum* induced differential expression of 15 transcription factors (Dataset S2), potentially indicating a widespread response beyond σ^E.

The sRNA FoxI Is a Negative Regulator of the σ^E Response. In previous work (17), we showed that the FoxI sRNA acted as a negative regulator of the abundant OM porin FomA. Although *fomA* did not pass our cutoff for significantly regulated transcripts (Fig. 3*A*), manual inspection of the global RNA-seq data revealed a clear decrease of *fomA* mRNA levels upon induced σ^E expression ($\log_2$ fold-change of -0.73). To test if FoxI might act as the negative regulator of σ^E in *F. nucleatum*, we used our *mazF*-based gene deletion tool pVoPo-04 to generate a Δ*foxI* strain (Fig. 5*A*). Following complementation of this strain with the inducible σ^E expression plasmid, we performed a global RNA-seq analysis after σ^E induction for 30 min. A comparison of down-regulated genes in the WT and the Δ*foxI* strain showed that *fomA* mRNA levels were not reduced when FoxI was absent (Dataset S1). Similarly, the Δ*foxI* strain failed to down-regulate *mglB* after σ^E expression (Fig. 5*B*), suggesting that the *mglB* mRNA might be another FoxI target. Nonetheless, *mglB* was the only other mRNA to show

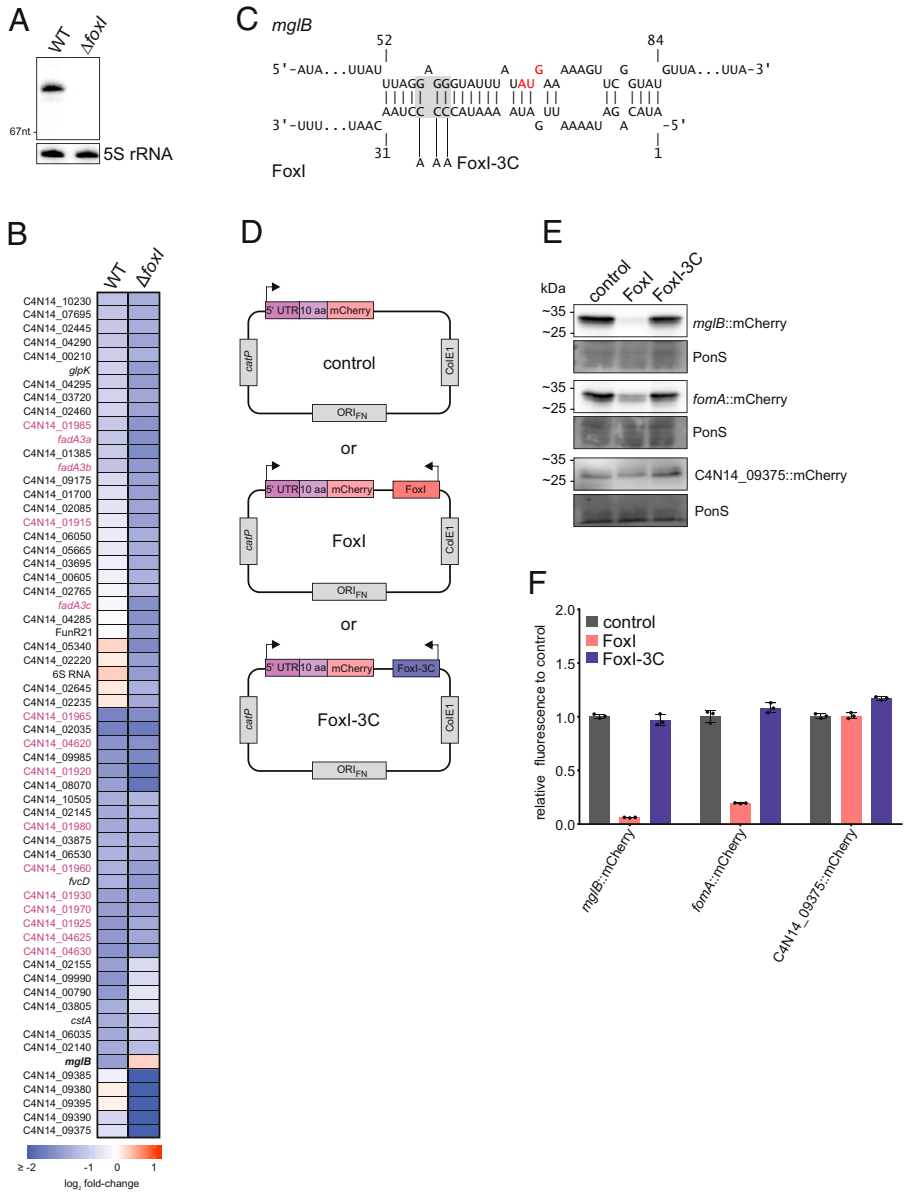

Fig. 5. The sRNA FoxI as a negative regulator of the σ^E response. (*A*) Northern blot detection of FoxI using total RNA samples extracted from *F. nucleatum* WT or Δ*foxI* generated via the deletion system pVoPo-04. The 5S rRNA served as loading control. (*B*) Differential gene expression upon σ^E induction in WT *F. nucleatum* or in the FoxI deletion strain (Δ*foxI*). The heatmap displays $\log_2$ fold-changes of genes that are significantly down-regulated in either background ($\log_2$ fold-change ≤ −1; FDR ≤ 0.05). *mglB* is marked in bold as the only gene that is not down-regulated in the Δ*foxI* background upon σ^E induction. Members of the three multicistronic operons started by FadA-domain containing genes are marked in purple. (*C*) Schematic representation of IntaRNA (93,) prediction of base-pairing between *mglB* mRNA and FoxI. The AUG start codon of *mglB* is marked in red. The mutation of the sRNA for FoxI-3C is indicated in gray. (*D*) Schematic representation of the translational reporter constructs used in *E*. *F. nucleatum* was either transformed with pVoPo-02 plasmids carrying mCherry fused to the 5′-region of the target gene only (control), or in combination with the expression cassette for FoxI (FoxI) or the seed region mutant FoxI-3C. (*E*) Representative western blots for each gene tested in the translational reporter system. C4N14_09375 served as control gene as it does not harbor any predicted FoxI-binding site. PonS staining is shown as loading control. (*F*) Quantification of mCherry by flow cytometry for the same constructs as shown in *E*. The average of three biological replicates relative to that of the control (control) is displayed together with the SD.

altered levels in the Δ*foxI* background, indicating that other targets of FoxI might be primarily regulated on the level of translation. Furthermore, additional σ^E-dependent sRNAs that compensate for FoxI function might be present, similar to what is seen in *E. coli* (38) and *V. cholerae* (40).

Posttranscriptional Repression of Envelope Protein MglB by FoxI. An in silico prediction of RNA interactions indicated a potential binding site of the FoxI sRNA across the Shine-Dalgarno sequence of *mglB* (Fig. 5*C*), expected to prevent MglB synthesis upon binding of the sRNA. To validate the *mglB* mRNA as a FoxI target, we constructed a translational reporter based on plasmid pVoPo-02, expressing the 5′ UTR and the first 10 aa of *mglB* as a fusion to mCherry from a constitutive promoter. Subsequently, we added expression cassettes for FoxI or a FoxI mutant that carries mutations in its seed region (FoxI-3C) (Fig. 5*D*). Western blot analysis showed a strong reduction of the MglB::mCherry protein in the presence of FoxI compared to the control (Fig. 5*E* and *SI Appendix*, Fig. S7*A*), similarly to a mCherry fusion of the known target *fomA*. We further confirmed this effect by quantification of the fluorescence signal of the mCherry fusions via flow cytometry (Fig. 5*F*). These interactions are likely mediated via direct base-pairing since coexpression of the seed region mutant FoxI-3C did not down-regulate these translational reporters (Fig. 5 *E* and *F*). No regulation was observed with a C4N14_09375::

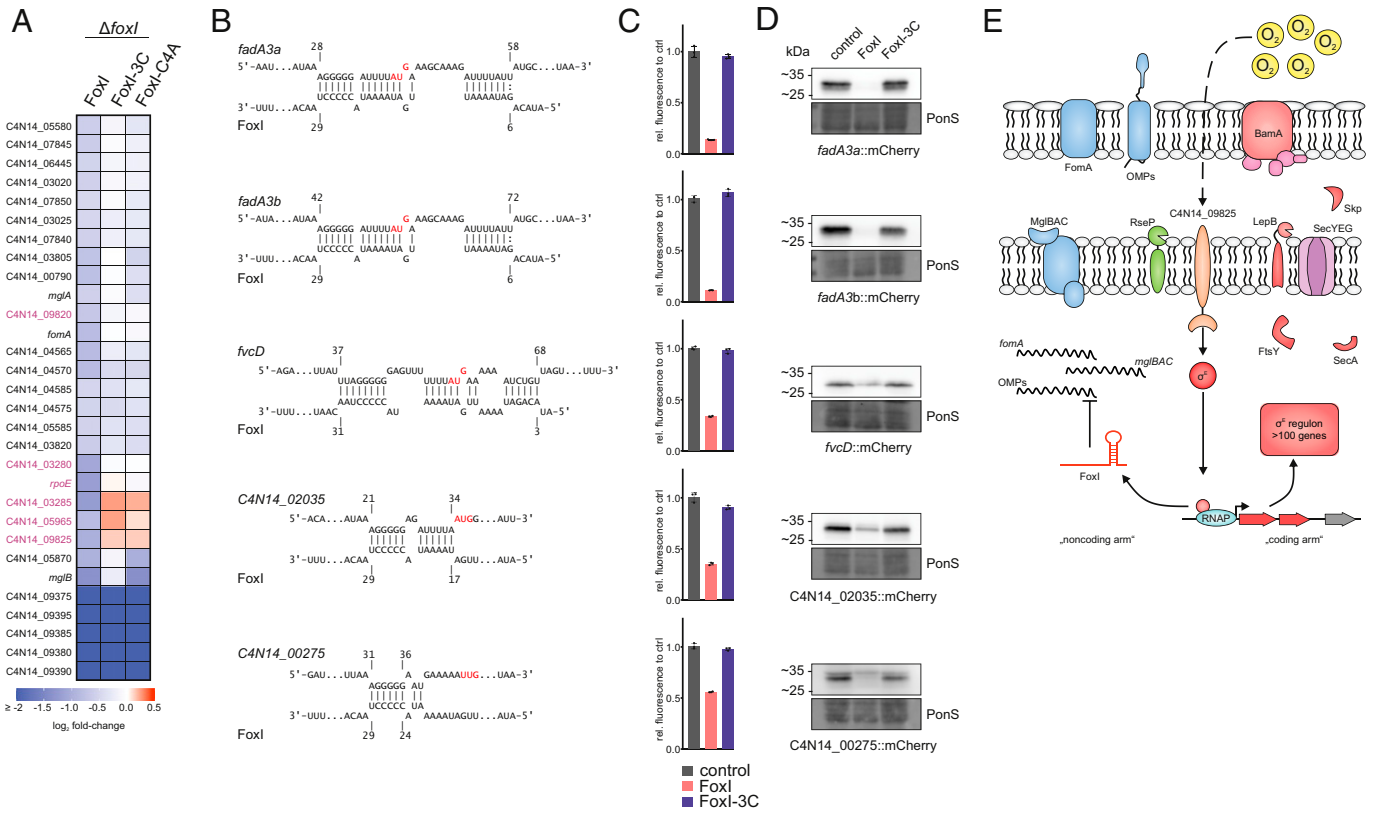

Fig. 6. Extended target spectrum of the FoxI sRNA. (*A*) Overview of all significantly down-regulated genes ($\log_2$ fold-change ≤ -0.5; FDR ≤ 0.05) upon pulse expression of FoxI or the seed region mutants FoxI-3C or FoxI-C4A in the Δ*foxI* background. The heatmap displays the $\log_2$ fold-changes. Genes of the identified σ^E regulon (Fig. 3) are marked in purple. (*B*) Schematic representation of IntaRNA target predictions between different target mRNAs and FoxI. The AUG start codons are marked in red. (*C*) Quantification of mCherry by flow cytometry for the translational reporter plasmids carrying the target 5′ region shown in *B* alone (control) or in the presence of FoxI or FoxI-3C. The average of three biological replicates relative to that of the control is displayed together with the SD. (*D*) Representative images of western blots of total protein samples for bacteria expressing the indicated reported constructs probed for mCherry. PonS staining is shown as loading control. (*E*) Model of the σ^E regulon in *F. nucleatum*. σ^E is released from its putative anti-σ factor (C4N14_09825) and up-regulates expression of its regulon consisting of >100 genes (marked in red). This includes *bamA* and *skp*, important for insertion of OMPs as well as *lepB*, *ftsY*, or *secA*, which are involved in protein-translocation across the IM. σ^E also activates the transcription of the sRNA FoxI. FoxI, in turn, down-regulates membrane-associated proteins such as the IM protein complex *mglBAC* and the OMP *fomA* as well as other OMPs.

mCherry fusion, chosen as a negative control since the C4N14_09375 mRNA does not harbor a predicted FoxI binding site. Combined, the results reveal *mglB* as a second target of the sRNA FoxI and highlight the application of our translational fusion system to validate sRNA-mediated mRNA regulation in *F. nucleatum*.

Global Transcriptome Changes Induced by FoxI Expression and sRNA Target Identification. Induced overexpression of sRNAs is a powerful approach to capture the targetome of sRNAs (42, 75, 76), which includes successful experimental target searches for σ^E-dependent sRNAs in Proteobacteria (37, 40, 42). Here, we took a similar approach and pulse-expressed FoxI, FoxI-3C, as well as FoxI-C4A, a mutant that carries only a single point mutation in the seed region, in the *F. nucleatum* Δ*foxI* strain for 20 min. Of note, under these experimental conditions, FoxI did not affect bacterial growth (*SI Appendix*, Fig. S2). RNA-seq identified 30 down-regulated mRNAs as potential FoxI targets ($-0.5 \leq \log_2$ fold-change ≥ 0.5; FDR ≤ 0.5); for most of these, repression was lost when expressing the seed region mutants FoxI-3C and FoxI-C4A (Fig. 6*A* and Dataset S3). The strongest negative regulation was observed for the C4N14_09375-C4N14_09395 operon of unknown function (Fig. 6*A*). However, this operon was also down-regulated by expression of the FoxI seed mutants, arguing against it being a direct target of FoxI. More importantly, we observed down-regulation of the FoxI target *mglB* and of *mglA*, the gene immediately downstream of *mglB* in the *mglBAC* operon. Curiously, pulse-expression of FoxI-C4A also reduced the *mglB* transcript levels but did not affect *fomA* mRNA (Fig. 6*A*), possibly indicating a more robust target interaction of FoxI with *mglB* in comparison to *fomA* (*SI Appendix*, Fig. S8). In addition, several genes of the σ^E regulon, including the σ^E operon itself, were down-regulated upon expression of a WT copy of FoxI, but not the seed mutants (Fig. 6*A*, purple). Interestingly, in silico target predictions for FoxI only revealed poor binding sites for these genes (Dataset S4), suggesting that some of them are regulated as an indirect consequence of FoxI-mediated relief of basal activation of σ^E. Overall, our analysis supports the identification of *mglB* as a direct target of the sRNA. Nevertheless, the moderate changes in RNA levels upon FoxI expression suggests that this sRNA might act primarily on the translational level, similar to the sRNA Spot 42 in *E. coli*, which blocks translation within the *galETKM* mRNA without affecting mRNA levels (77).

Evidence for Multitarget Regulation by the FoxI sRNA. In *E. coli*, the σ^E-dependent sRNAs MicA, RybB, and MicL repress the mRNAs of several OMPs as well as the abundant Lpp protein (37, 38, 42). Since unfolded OMPs and Lpp are potent triggers of σ^E, the sRNA-mediated translational inhibition results in a negative feedback-loop within the σ^E response. Interestingly, we observed repression for several OMPs upon σ^E induction in *F. nucleatum* (Fig. 3) and in silico target prediction indicates

promising binding sites for FoxI for some of these OMPs (Fig. 6*B* and Dataset S3). We therefore hypothesized that FoxI might block the synthesis of multiple OMPs without directly affecting their RNA levels. To test this, we applied our translational reporter system to five additional candidate target mRNAs, whose levels decreased upon σ^E induction: *fadA*2, *fadA*3, *fvcD*, C4N14_00275, and C4N14_02035. In all of these cases we observed a strong translational repression upon constitutive FoxI expression, but not upon expression of the FoxI-3C mutant measured by flow cytometry (Fig. 6*C*) and western blot analysis (Fig. 6*D* and *SI Appendix*, Fig. S7*B*). Thus, we have obtained evidence for FoxI-mediated posttranscriptional repression of at least seven mRNAs of envelope proteins, lending further support to a model in which the conserved FoxI sRNA acts as the global noncoding arm of the fusobacterial σ^E response (Fig. 6*E*).

Discussion

Despite the growing appreciation of their importance for health and disease, the vast majority of the >4,500 bacterial species that constitute the human microbiota are currently molecular *terra incognita* (78). Research in this area is hampered by the fact that genetic modification of these bacteria is notoriously difficult and thus we lack the ability to genetically dissect their physiology and molecular principles of gene regulation. *F. nucleatum* has emerged as a new paradigm for such microbes and its ability to colonize distal body sites has increasingly been recognized as a medical problem (2). Here, we present a broad suite of genetic tools for *F. nucleatum* and apply these to uncover a conserved stress response mediated by the ECF σ^E in this bacterium, which was triggered by oxygen instead of general envelope perturbation.

Our present knowledge of the architecture of the σ^E response primarily stems from studies in a few γ-proteobacterial species (30), were it was shown to be a central player in combatting envelope stress. σ^E up-regulates factors that ensure proper folding and insertion of OMPs or lipoproteins and thereby helps to maintain and shape the bacterial envelope. Since *F. nucleatum* exhibits a very large phylogenetic distance to these proteobacterial species (14), it was surprising to discover in *F. nucleatum* a σ^E regulon of similar architecture to *E. coli* (31, 38): many of the genes controlled by σ^E possess envelope-related functions, and there is a noncoding arm (i.e., the FoxI sRNA), many of whose target mRNAs also encode proteins with envelope-related functions. Strikingly, however, σ^E itself is not induced by known triggers of envelope stress but by exposure to oxygen. While the molecular mechanism of oxygen-mediated activation remains to be elucidated, it is tempting to speculate that σ^E in this early-branching anaerobic bacterium serves the role of an environmental sensor, while sharing the envelope remodeling function with *E. coli* σ^E.

As to specific σ^E-controlled genes, *skp* (79) and *bamA* (66) encode proteins that work cooperatively to ensure proper insertion of unfolded OMPs into the OM. The protein encoded by *lpxD*, on the other hand, is integral for liposaccharide biosynthesis (80), another important component of the envelope of gram-negative bacteria. We also identified a consensus σ^E-binding site, consisting of the conserved −10 and −35 boxes, similar to *E. coli* and *P. aeruginosa* (31, 62). In light of the evolutionary distance between Fusobacteriota and other bacterial phyla (14), this conservation suggests that the σ^E response represents a very deeply rooted regulon that maintains bacterial envelope homeostasis. The σ^E regulon in *F. nucleatum* also includes genes encoding three integral members of the Sec-dependent protein translocation pathway: *ftsY*, *secA*, and *lepB*. The FtsY and SecA proteins facilitate the translocation process, in a cotranslational or posttranslational manner, respectively. The signal peptidase LepB releases translocated proteins into the periplasm (81). Interestingly, these proteins have not been found to be under σ^E control in other bacteria, but increased translocation capacity would be expected to act in synergy with enhanced OMP insertion. After all, the Sec-pathway is the major transport mechanism for OMPs to the periplasm (81, 82). Although we still lack a functional understanding of the 117 genes that are part of the σ^E regulon in *F. nucleatum*, it is clear that at least part of the physiological role of σ^E in this anaerobic bacterium is envelope maintenance, reflecting a core function for this ECF.

The link between σ^E and the response to molecular oxygen is supported by the common activation of 23 genes upon σ^E induction and oxygen exposure (Fig. 4). An interesting example is activation of the dicistronic operon *ccdA-msrAB*, which is paralogues to an operon previously linked to the defense against hydrogen peroxide in *F. nucleatum* (Dataset S1) (13). Thus, the σ^E regulon in *F. nucleatum* might serve a dual function by neutralizing oxygen and by modulating the bacterial envelope, acting in synergy in this anaerobe bacterium. However, based on the differential expression of 15 transcription factors, it is clear that σ^E is not the only mediator of an oxygen-induced response. Therefore, it will be important to understand how this anaerobe senses oxygen and transmits the signal to activate σ^E. As to the actual activation mechanism, we note that *F. nucleatum* has no homolog of the protease DegS, which senses unfolded OMPs in *E. coli* (83). DegS initiates a proteolytic cascade that leads to the degradation of the anti-σ factor and release of σ^E (84, 85). The lack of DegS might imply that *F. nucleatum* uses alternative ways of perceiving and relaying stress signals that lead to σ^E activation. These might involve phosphorylation as shown for the *Vibrio parahaemolyticus* σ factor EcfP (27) or a TCS, as seen during activation of SigE in *Streptomyces coelicolor* (28). Interestingly, the fusobacterial TCS ModRS was recently shown to be involved in the response to H_2O_2 (13). However, ModRS is not activated by oxygen (Dataset S3). Alternatively, the anti-σ factor could be directly involved in sensing oxygen and subsequently trigger σ^E activation. Such a mechanism has been shown for singlet oxygen in *Rhodobacter sphaeroides*, where the anti-σ factor ChrR directly responds to the reactive oxygen species and releases σ^E (21, 24, 86). Another possibility is activation via cofactors, such as $[4Fe\text{-}S]^{2+}$ or heme, which present widespread oxygen-sensing mechanisms in bacteria (87).

One of the most striking findings of the σ^E response of *F. nucleatum* is the conservation of a noncoding repressor arm, constituted by the sRNA FoxI, in an organism that lacks known sRNA chaperones. Although sRNAs are frequently part of regulatory circuits, there is only one example of broad conservation in different phyla: the sRNAs controlled by the iron uptake regulator Fur (88). Fur is present in gram-positive and gram-negative bacteria because iron is essential for all bacteria (89). The Fur-dependent sRNAs, such as RyhB in *E. coli* (90), expand Fur's transcriptional repressor function upon iron starvation (91, 92). Similarly, sRNAs form the repressive arm of the σ^E response and play an important role in downregulating envelope proteins (38). However, evidence for a conservation of this function has come from the single phylum of Proteobacteria (i.e., from *E. coli* and *Salmonella*) (39, 42, 49, 69), *P. aeruginosa* (70), and *Vibrio cholerae* (40, 41). Here, we find that the sRNA FoxI is expressed in a σ^E-dependent fashion and represses the translation of the OM porin FomA, the MglBAC galactose-uptake system and leading genes of operons that encode type 5a autotransporters, another class of abundant

fusobacterial OMPs (12, 94–96). Our observations suggest that FoxI reduces translation of membrane proteins, thereby limiting the burden on the Sec- and BAM-dependent membrane protein insertion pathways. This is likely also reflected in the observation that expression of FoxI in the Δ*foxI* background decreases expression of the *rpoE* and C4N14_03280-C4N14_03285 operons (Fig. 6*A*), which might indicate a decreased activation of the basal σ^E stress response. FoxI and σ^E thus work synergistically to maintain envelope homeostasis and integrity in *F. nucleatum* (Fig. 6*E*), mirroring the coding arm and noncoding arm principle established by σ^E-dependent sRNAs in *E. coli* (38). Nevertheless, the fact that we did not observe a strict dependence of σ^E-repressed targets on FoxI suggests that there could be additional σ^E-dependent sRNAs. This has been seen in *E. coli* (MicA, RybB) (38) or *V. cholerae* (VrrA, MicV) (40), where two sRNAs share common targets and compensate for another.

As mentioned, all σ^E-dependent sRNAs studied thus far rely on the RNA chaperone Hfq for their activity (42, 46, 49), but *F. nucleatum* lacks known sRNA chaperones. It nevertheless remains possible that a yet unidentified RNA-binding protein (RBP) plays a role in sRNA-mediated regulation in *F. nucleatum*. To facilitate the discovery of such RBPs, proteins interacting with FoxI could be identified using the sRNA as bait for pulldown experiments (76). A promising candidate for this role might be the RBP KhpB, which has been found to bind RNA in *Streptococcus pneumonia* and *Clostridium difficile* (97–99), and for which *F. nucleatum* harbors a homolog.

Overall, our study highlights the conservation of the regulatory principle of the bacterial σ^E response, despite the evolutionary distance of Fusobacteria to other bacterial clades, and provides much-needed tools to dissect *F. nucleatum* gene function in order to accelerate research into this clinically relevant bacterium.

Materials and Methods

Strains and Growth Conditions. All oligonucleotides, plasmids, or strains used in the present study can be found in Dataset S5. *F. nucleatum* subspecies *nucleatum* ATCC 23726 was acquired from the American Type Culture Collection (ATCC). *F. nucleatum* was routinely grown at 37 °C in 80:10:10 (N_2:H_2:CO_2) on 2% agar BHI-C plates (brain–heart infusion [BHI], 1% [w:v] yeast extract, 1% [w:v] glucose, 5 μg mL^{-1} of hemin; 1% [v:v] fetal bovine serum). For liquid growth Columbia broth medium was utilized. For selecting *F. nucleatum* carrying a plasmid or for selection steps during gene deletion, BHI-C agar plates were supplemented with 5 μg mL^{-1} thiamphenicol and liquid cultures with 2.5 μg mL^{-1} of the antibiotic. For details regarding the transformation, see *SI Appendix, Material and Methods*. All solutions or plates were always prereduced overnight prior to use in the anaerobic chamber to ensure the absence of entrapped oxygen. For growing *F. nucleatum*, precultures were prepared 24 h prior to inoculating the working cultures (1:50 dilution).

Construction of pVoPo and Related Plasmids. Comprehensive descriptions for the construction of the different constructs used in this study are provided in *SI Appendix, Material and Methods*.

Evaluation of MazF Expression for Counterselection. To create a *mazF*-containing plasmid that allows replication in *F. nucleatum*, the ORI_{FN} was inserted into the PvuI and NotI site of pVoPo-02 generating pVoPo-01-*mazF* (p.*mazF*). Subsequently, bacteria carrying p.*mazF* or the control vector pVoPo-01 (p.empty) were used to prepare precultures in biological triplicates. For analysis of bacterial survival, the cells were grown to mid-exponential phase and exposed to either 100 ng mL^{-1} ATc or left untreated. Serial dilutions were plated at 0 min, 30 min, or 3 h after treatment. For this, 10 μL were spotted in technical triplicates on BHI-C plates. Three days later, all technical replicates for the appropriate dilutions were counted and averaged for each biological replicate. The average and SD are shown in Fig. 2*D*. For analysis of growth, precultures for three replicates were diluted as described above either in the presence of 100 ng mL^{-1} ATc or left untreated. Growth was monitored for 24 h using a plate reader and reported as the average of three biological replicates for each group in Fig. 2*D*.

Generating Clean Deletion Mutant Using pVoPo-04 System. To allow homologous recombination, 1-kB flanking up- and downstream of the target gene were amplified from genomic DNA of *F. nucleatum* and assembled in pVoPo-04 as described above. Transformation was carried out as described above and successful integration events were restreaked on fresh BHI-C plates containing thiamphenicol. Colonies that grew had successfully integrated the suicide vector into the genome (marked as first recombination). A single colony was used to inoculate an overnight culture in Columbia broth without selection pressure to allow the second recombination step to take place. The next day, the culture was diluted 1:50 into media containing 100 ng mL^{-1} ATc. This allows for the counterselection due to the toxic expression of the toxin MazF and only bacteria having lost the plasmid can grow. After 4 h, serial dilutions were plated on BHI-C plates. The loss of the plasmid was verified via restreaking resulting colonies on BHI-C and BHI-C–containing thiamphenicol plates. Only colonies growing on BHI-C but not the plates with antibiotic were used for further validation via PCR to check for the loss of the target gene or reversion to the WT.

Northern and Western Blot Detection. For further experimental details on the northern and western blots, see *SI Appendix, Material and Methods*.

Sample Collection for RNA-Seq of σ^E Expression. Three biological replicates for each group (WT: p.empty; p.*rpoE* and Δ*foxI*: p.empty; p.*rpoE*) were grown to mid-exponential phase. All samples were induced with 100 ng mL^{-1} of ATc for 30 min. Samples were fixed by adding STOP Mix (95% [v:v] EtOH; 5% [v:v] phenol) and then snap-frozen in liquid nitrogen. Samples were stored at −80 °C until further processing. The Hot Phenol was used for RNA extraction as reported previously (17).

Analysis of Fluorescent Protein Expression by Confocal Microscopy. *F. nucleatum* carrying the individual pVoPo-FP plasmids were grown to mid-exponential phase. All of the following steps were conducted outside the anaerobic chamber. One milliliter of each culture was spun down and washed once in PBS. Next, the bacteria were fixed in 4% (w/V) PFA for 20 min at 4 °C. Afterward, the cells were washed once with PBS prior to overnight incubation in PBS at 4 °C. This step ensures proper maturation of the fluorescent proteins. The next day, the samples were imaged on ibdi chambered coverslips performed on a Leica SP5 laser scanning confocal microscope (Leica Microsystems) acquiring the fluorescence signal at the indicated wave lengths.

Exposure of *F. nucleatum* to Different Stress Conditions. Three biological replicates of *F. nucleatum* were grown to mid-exponential phase. The cultures were split into 3-mL aliquots and treated by adding a 1 mL of a 4× solution in Columbia broth of the following conditions for 60 min: polymyxin B (400 ng mL^{-1}), lysozyme (125 μg mL^{-1}), NaCl (600 mM), bile (0.05% (w/V), H_2O_2 (400 μM), diamide (125 μM), GNSO (250 μM), mitomycin C (625 ng mL^{-1}). The final concentrations used are given. For the heat shock, the samples were placed in an incubator at 42 °C for the duration of the treatment. Regarding the oxygen exposure, the samples were poured into a Petri dish and placed in an incubator at 37 °C outside of the anaerobic chamber for the duration of the treatment. One milliliter of Columbia broth was added as a control to untreated to the control samples. After 60 min, samples were fixed through the addition of STOP mix and RNA extracted via the Hot Phenol protocol, as mentioned above.

Gene-Expression Analysis via qRT-PCR. One microgram of DNase-digested RNA was used as input to generate cDNA using the M-MLV reverse transcriptase (ThermoFisher Scientific) and random hexamer primers following the manufacturer's instructions. The equivalent of 10 ng RNA was used for qPCR analysis using gene specific primers (Dataset S5). For this, the Takyon Master Mix was used according to the manufacturer's protocol. The relative fold-changes to the control were calculated based upon the $2^{-\Delta\Delta Ct}$ method (100). The 5S rRNA was used as reference gene.

Sample Collection and Analysis for Translation Fusion Experiments by Western Blot. *F. nucleatum* carrying the individual translational fusion alone, or in combination with FoxI/FoxI-3C was grown to mid-exponential phase and cells were quickly spun down and snap-frozen in liquid nitrogen. Thawed cells were resuspended in protein loading buffer and 0.2 $OD_{600\ nm}$ units were used for western blot analysis. Quantification of the fusion products signal in the western blot was carried out using ImageJ (101). Three biological replicates were analyzed in each case and the average together with the SD reported.

Sample Collection and Analysis for Translation Fusion Experiments by Flow Cytometry. *F. nucleatum* carrying the individual translational fusion alone, or in combination with FoxI/FoxI-3C, was grown to mid-exponential phase and cells spun down for 3 min at 4,000 × *g*. This and all following steps were conducted outside of the anaerobic chamber. After removing the supernatant, the bacteria were fixated in 4% (w/V) PFA for 20 min at 4 °C. Next, the cells were washed with 1× PBS before incubating them with DAPI in PBS (100 ng mL^{-1}) for 5 min at room temperature. The bacteria were washed once more with PBS and resuspended in PBS. To ensure full maturation of the fluorescent protein, the samples were left overnight at 4 °C. The next day, the fluorescence intensity was measured by flow cytometry at 615 to 620 nm for 50,000 cells of each sample determined by a $DAPI^+$ signal.

Sample Collection and Analysis for Transcriptional Reporter Experiments. *F. nucleatum* carrying the individual transcriptional reporters was grown to mid-exponential phase. At this time, samples were collected and snap-frozen. No quantification was carried out as no signal could be detected for samples with the point mutation.

Sample Collection for RNA-Seq of sRNA Expression. Three biological replicates for each group (Δ*foxI*: p.empty; FoxI; FoxI-3C; FoxI-C4A) were grown to mid-exponential phase. All samples were induced with 100 ng mL^{-1} of ATc for 20 min. Samples were treated as described above prior to performing RNA extraction according to the Hot Phenol protocol.

Sample Collection for RNA-Seq upon Oxygen and Polymyxin B Exposure. Three biological replicates of WT *F. nucleatum* were grown to mid-exponential growth phase. The cultures were exposed either to atmospheric oxygen concentrations outside of the anaerobic chamber (maintaining 37 °C) or treated with 400 ng mL^{-1} of polymyxin B for 20 min. Untreated samples were used as control. RNA extraction was performed according to the Hot Phenol protocol.

Analysis of RNA-Seq Data. A detailed description for the analysis of all RNA-seq data can be found in the *SI Appendix, Material and Methods*.

Promoter Analysis. For the identification of promoter motif, each significantly up-regulated gene resulting from the σ^E expression was grouped into transcriptional units (Fig. 3*A*). Based on our previous data for the TSS (17), we then extracted 50 nt upstream of each TSS for the individual transcriptional unit. Internal as well as secondary start sites of genes where we observed strong RNA-seq up-regulation were treated the same. These nucleotide sequences were used as input for analysis via MEME (v4.12.0) (102).

Data, Materials, and Software Availability. The data reported in this paper have been deposited in the Gene Expression Omnibus (GEO) database, https://www.ncbi.nlm.nih.gov/geo (accession no. GSE192339) (103). Plasmids pVoPo-GFP–pVoPo-mNG (104–107,) (with the individual fluorescence proteins) and pVoPo-01–pVoPo-04 (108–111) have been deposited with Addgene (Dataset S5).

ACKNOWLEDGMENTS. We thank Anke Sparmann for her helpful comments on and editing of the manuscript; Anna Nöhren and Esther Hauschild for their excellent technical assistance; Svetlana Đurica-Mitić, Kotaro Chihara, and Gianluca Matera for helpful comments and discussion; and the Vogel Stiftung Dr. Eckernkamp for supporting F.P. and V.C. with a Dr. Eckernkamp Fellowship. This work was supported by funds to J.V. from a Deutsche Forschungsgemeinschaft Gottfried Wilhelm Leibniz Award (DFG Vo875-18) and the Bavarian bayresq.net project Rbiotics.

1. A. L. Griffen *et al.*, Distinct and complex bacterial profiles in human periodontitis and health revealed by 16S pyrosequencing. *ISME J.* **6**, 1176–1185 (2012).
2. C. A. Brennan, W. S. Garrett, Fusobacterium nucleatum–Symbiont, opportunist and oncobacterium. *Nat. Rev. Microbiol.* **17**, 156–166 (2019).
3. P. E. Kolenbrander, Oral microbial communities: Biofilms, interactions, and genetic systems. *Annu. Rev. Microbiol.* **54**, 413–437 (2000).
4. Y. W. Han, Fusobacterium nucleatum: A commensal-turned pathogen. *Curr. Opin. Microbiol.* **23**, 141–147 (2015).
5. A. D. Kostic *et al.*, Genomic analysis identifies association of Fusobacterium with colorectal carcinoma. *Genome Res.* **22**, 292–298 (2012).
6. M. Castellarin *et al.*, Fusobacterium nucleatum infection is prevalent in human colorectal carcinoma. *Genome Res.* **22**, 299–306 (2012).
7. D. Nejman *et al.*, The human tumor microbiome is composed of tumor type-specific intracellular bacteria. *Science* **368**, 973–980 (2020).
8. K. Yamamura *et al.*, Human microbiome fusobacterium nucleatum in esophageal cancer tissue is associated with prognosis. *Clin. Cancer Res.* **22**, 5574–5581 (2016).
9. T. Yu *et al.*, *Fusobacterium nucleatum* promotes chemoresistance to colorectal cancer by modulating autophagy. *Cell* **170**, 548–563.e16 (2017).
10. S. Bullman *et al.*, Analysis of *Fusobacterium* persistence and antibiotic response in colorectal cancer. *Science* **358**, 1443–1448 (2017).
11. L. Parhi *et al.*, Breast cancer colonization by Fusobacterium nucleatum accelerates tumor growth and metastatic progression. *Nat. Commun.* **11**, 3259 (2020).
12. C. Wu *et al.*, Genetic and molecular determinants of polymicrobial interactions in *Fusobacterium nucleatum*. *Proc. Natl. Acad. Sci. U.S.A.* **118**, e2006482118 (2021).
13. M. Scheible *et al.*, The fused methionine sulfoxide reductase MsrAB promotes oxidative stress defense and bacterial virulence in *Fusobacterium nucleatum*. *mBio* **13**, e0302221 (2022).
14. G. A. Coleman *et al.*, A rooted phylogeny resolves early bacterial evolution. *Science* **372**, eabe0511 (2021).
15. C. Wu *et al.*, Forward genetic dissection of biofilm development by *Fusobacterium nucleatum*: Novel functions of cell division proteins FtsX and EnvC. *mBio* **9**, e00360-18 (2018).
16. M. A. Casasanta *et al.*, *Fusobacterium nucleatum* host-cell binding and invasion induces IL-8 and CXCL1 secretion that drives colorectal cancer cell migration. *Sci. Signal.* **13**, eaba9157 (2020).
17. F. Ponath *et al.*, RNA landscape of the emerging cancer-associated microbe Fusobacterium nucleatum. *Nat. Microbiol.* **6**, 1007–1020 (2021).
18. A. Staroń *et al.*, The third pillar of bacterial signal transduction: Classification of the extracytoplasmic function (ECF) sigma factor protein family. *Mol. Microbiol.* **74**, 557–581 (2009).
19. J. D. Helmann, The extracytoplasmic function (ECF) sigma factors. *Adv. Microb. Physiol.* **46**, 47–110 (2002).
20. G. Rowley, M. Spector, J. Kormanec, M. Roberts, Pushing the envelope: Extracytoplasmic stress responses in bacterial pathogens. *Nat. Rev. Microbiol.* **4**, 383–394 (2006).
21. J. R. Anthony, K. L. Warczak, T. J. Donohue, A transcriptional response to singlet oxygen, a toxic byproduct of photosynthesis. *Proc. Natl. Acad. Sci. U.S.A.* **102**, 6502–6507 (2005).
22. T. D. Ho, C. D. Ellermeier, Activation of the extracytoplasmic function σ factor σ^V by lysozyme. *Mol. Microbiol.* **112**, 410–419 (2019).
23. I. L. Grigorova *et al.*, Fine-tuning of the Escherichia coli sigmaE envelope stress response relies on multiple mechanisms to inhibit signal-independent proteolysis of the transmembrane anti-sigma factor, RseA. *Genes Dev.* **18**, 2686–2697 (2004).
24. E. A. Campbell *et al.*, A conserved structural module regulates transcriptional responses to diverse stress signals in bacteria. *Mol. Cell* **27**, 793–805 (2007).
25. K. V. Rajasekar *et al.*, The anti-sigma factor RsrA responds to oxidative stress by reburying its hydrophobic core. *Nat. Commun.* **7**, 12194 (2016).
26. A. Francez-Charlot *et al.*, Sigma factor mimicry involved in regulation of general stress response. *Proc. Natl. Acad. Sci. U.S.A.* **106**, 3467–3472 (2009).
27. S. C. Iyer *et al.*, Transcriptional regulation by σ factor phosphorylation in bacteria. *Nat. Microbiol.* **5**, 395–406 (2020).
28. M. S. Paget, E. Leibovitz, M. J. Buttner, A putative two-component signal transduction system regulates sigmaE, a sigma factor required for normal cell wall integrity in Streptomyces coelicolor A3(2). *Mol. Microbiol.* **33**, 97–107 (1999).
29. J. W. Erickson, C. A. Gross, Identification of the sigma E subunit of *Escherichia coli* RNA polymerase: A second alternate sigma factor involved in high-temperature gene expression. *Genes Dev.* **3**, 1462–1471 (1989).
30. C. L. Hews, T. Cho, G. Rowley, T. L. Raivio, Maintaining integrity under stress: Envelope stress response regulation of pathogenesis in gram-negative bacteria. *Front. Cell. Infect. Microbiol.* **9**, 313 (2019).
31. V. A. Rhodius, W. C. Suh, G. Nonaka, J. West, C. A. Gross, Conserved and variable functions of the sigmaE stress response in related genomes. *PLoS Biol.* **4**, e2 (2006).
32. H. Skovierova *et al.*, Identification of the sigmaE regulon of *Salmonella enterica* serovar Typhimurium. *Microbiology (Reading)* **152**, 1347–1359 (2006).
33. C. Dartigalongue, D. Missiakas, S. Raina, Characterization of the *Escherichia coli* sigma E regulon. *J. Biol. Chem.* **276**, 20866–20875 (2001).
34. S. E. Ades, Regulation by destruction: Design of the sigmaE envelope stress response. *Curr. Opin. Microbiol.* **11**, 535–540 (2008).
35. V. K. Mutalik, G. Nonaka, S. E. Ades, V. A. Rhodius, C. A. Gross, Promoter strength properties of the complete sigma E regulon of *Escherichia coli* and *Salmonella enterica*. *J. Bacteriol.* **191**, 7279–7287 (2009).
36. K. S. Fröhlich, S. Gottesman, Small regulatory RNAs in the enterobacterial response to envelope damage and oxidative stress. *Microbiol. Spectr.* **6**, 10.1128/microbiolspec.RWR-0022-2018 (2018).
37. M. S. Guo *et al.*, MicL, a new σE-dependent sRNA, combats envelope stress by repressing synthesis of Lpp, the major outer membrane lipoprotein. *Genes Dev.* **28**, 1620–1634 (2014).
38. E. B. Gogol, V. A. Rhodius, K. Papenfort, J. Vogel, C. A. Gross, Small RNAs endow a transcriptional activator with essential repressor functions for single-tier control of a global stress regulon. *Proc. Natl. Acad. Sci. U.S.A.* **108**, 12875–12880 (2011).
39. J. Johansen, A. A. Rasmussen, M. Overgaard, P. Valentin-Hansen, Conserved small non-coding RNAs that belong to the sigmaE regulon: Role in down-regulation of outer membrane proteins. *J. Mol. Biol.* **364**, 1–8 (2006).
40. N. Peschek, M. Hoyos, R. Herzog, K. U. Förstner, K. Papenfort, A conserved RNA seed-pairing domain directs small RNA-mediated stress resistance in enterobacteria. *EMBO J.* **38**, e101650 (2019).

41. T. Song *et al.*, A new Vibrio cholerae sRNA modulates colonization and affects release of outer membrane vesicles. *Mol. Microbiol.* **70**, 100–111 (2008).
42. K. Papenfort *et al.*, SigmaE-dependent small RNAs of Salmonella respond to membrane stress by accelerating global omp mRNA decay. *Mol. Microbiol.* **62**, 1674–1688 (2006).
43. K. Papenfort, M. Bouvier, F. Mika, C. M. Sharma, J. Vogel, Evidence for an autonomous 5′ target recognition domain in an Hfq-associated small RNA. *Proc. Natl. Acad. Sci. U.S.A.* **107**, 20435–20440 (2010).
44. R. Balbontín, F. Fiorini, N. Figueroa-Bossi, J. Casadesús, L. Bossi, Recognition of heptameric seed sequence underlies multi-target regulation by RybB small RNA in Salmonella enterica. *Mol. Microbiol.* **78**, 380–394 (2010).
45. K. I. Udekwu, E. G. Wagner, Sigma E controls biogenesis of the antisense RNA MicA. *Nucleic Acids Res.* **35**, 1279–1288 (2007).
46. N. Figueroa-Bossi *et al.*, Loss of Hfq activates the sigmaE-dependent envelope stress response in Salmonella enterica. *Mol. Microbiol.* **62**, 838–852 (2006).
47. E. Guisbert, V. A. Rhodius, N. Ahuja, E. Witkin, C. A. Gross, Hfq modulates the sigmaE-mediated envelope stress response and the sigma32-mediated cytoplasmic stress response in Escherichia coli. *J. Bacteriol.* **189**, 1963–1973 (2007).
48. Y. Ding, B. M. Davis, M. K. Waldor, Hfq is essential for Vibrio cholerae virulence and downregulates sigma expression. *Mol. Microbiol.* **53**, 345–354 (2004).
49. K. M. Thompson, V. A. Rhodius, S. Gottesman, SigmaE regulates and is regulated by a small RNA in Escherichia coli. *J. Bacteriol.* **189**, 4243–4256 (2007).
50. V. Kapatral *et al.*, Genome sequence and analysis of the oral bacterium Fusobacterium nucleatum strain ATCC 25586. *J. Bacteriol.* **184**, 2005–2018 (2002).
51. D. Casas-Pastor *et al.*, Expansion and re-classification of the extracytoplasmic function (ECF) σ factor family. *Nucleic Acids Res.* **49**, 986–1005 (2021).
52. R. Lutz, H. Bujard, Independent and tight regulation of transcriptional units in Escherichia coli via the LacR/O, the TetR/O and AraC/I1-I2 regulatory elements. *Nucleic Acids Res.* **25**, 1203–1210 (1997).
53. P. Carroll, J. Muwanguzi-Karugaba, E. Melief, M. Files, T. Parish, Identification of the translational start site of codon-optimized mCherry in Mycobacterium tuberculosis. *BMC Res. Notes* **7**, 366 (2014).
54. S. Kinder Haake, S. Yoder, S. H. Gerardo, Efficient gene transfer and targeted mutagenesis in Fusobacterium nucleatum. *Plasmid* **55**, 27–38 (2006).
55. Y. W. Han *et al.*, Identification and characterization of a novel adhesin unique to oral fusobacteria. *J. Bacteriol.* **187**, 5330–5340 (2005).
56. C. W. Kaplan *et al.*, Fusobacterium nucleatum outer membrane proteins Fap2 and RadD induce cell death in human lymphocytes. *Infect. Immun.* **78**, 4773–4778 (2010).
57. C. W. Kaplan *et al.*, Fusobacterium nucleatum apoptosis-inducing outer membrane protein. *J. Dent. Res.* **84**, 700–704 (2005).
58. W. F. Van Zyl, L. M. T. Dicks, S. M. Deane, Development of a novel selection/counter-selection system for chromosomal gene integrations and deletions in lactic acid bacteria. *BMC Mol. Biol.* **20**, 10 (2019).
59. X. Z. Zhang, X. Yan, Z. L. Cui, Q. Hong, S. P. Li, mazF, a novel counter-selectable marker for unmarked chromosomal manipulation in Bacillus subtilis. *Nucleic Acids Res.* **34**, e71 (2006).
60. M. A. Al-Hinai, A. G. Fast, E. T. Papoutsakis, Novel system for efficient isolation of Clostridium double-crossover allelic exchange mutants enabling markerless chromosomal gene deletions and DNA integration. *Appl. Environ. Microbiol.* **78**, 8112–8121 (2012).
61. V. A. Rhodius, V. K. Mutalik, Predicting strength and function for promoters of the Escherichia coli alternative sigma factor, sigmaE. *Proc. Natl. Acad. Sci. U.S.A.* **107**, 2854–2859 (2010).
62. S. Schulz *et al.*, Elucidation of sigma factor-associated networks in Pseudomonas aeruginosa reveals a modular architecture with limited and function-specific crosstalk. *PLoS Pathog.* **11**, e1004744 (2015).
63. P. E. Rouvière *et al.*, rpoE, the gene encoding the second heat-shock sigma factor, sigma E, in Escherichia coli. *EMBO J.* **14**, 1032–1042 (1995).
64. M. S. Anderson, C. E. Bulawa, C. R. Raetz, The biosynthesis of gram-negative endotoxin. Formation of lipid A precursors from UDP-GlcNAc in extracts of Escherichia coli. *J. Biol. Chem.* **260**, 15536–15541 (1985).
65. J. G. Sklar, T. Wu, D. Kahne, T. J. Silhavy, Defining the roles of the periplasmic chaperones SurA, Skp, and DegP in Escherichia coli. *Genes Dev.* **21**, 2473–2484 (2007).
66. T. J. Knowles, A. Scott-Tucker, M. Overduin, I. R. Henderson, Membrane protein architects: The role of the BAM complex in outer membrane protein assembly. *Nat. Rev. Microbiol.* **7**, 206–214 (2009).
67. R. E. Dalbey, W. Wickner, Leader peptidase catalyzes the release of exported proteins from the outer surface of the Escherichia coli plasma membrane. *J. Biol. Chem.* **260**, 15925–15931 (1985).
68. R. Steinberg, L. Knüpffer, A. Origi, R. Asti, H. G. Koch, Co-translational protein targeting in bacteria. *FEMS Microbiol. Lett.* **365**, 10.1093/femsle/fny095 (2018).
69. K. I. Udekwu *et al.*, Hfq-dependent regulation of OmpA synthesis is mediated by an antisense RNA. *Genes Dev.* **19**, 2355–2366 (2005).
70. S. Ferrara *et al.*, Post-transcriptional regulation of the virulence-associated enzyme AlgC by the σ(22) -dependent small RNA ErsA of Pseudomonas aeruginosa. *Environ. Microbiol.* **17**, 199–214 (2015).
71. S. Campagne, M. E. Marsh, G. Capitani, J. A. Vorholt, H.-T. Allain, Structural basis for −10 promoter element melting by environmentally induced sigma factors. *Nat. Struct. Mol. Biol.* **21**, 269–276 (2014).
72. J. Mecsas, P. E. Rouviere, J. W. Erickson, T. J. Donohue, C. A. Gross, The activity of sigma E, an Escherichia coli heat-inducible sigma-factor, is modulated by expression of outer membrane proteins. *Genes Dev.* **7**, 2618–2628 (1993).
73. T. L. Testerman *et al.*, The alternative sigma factor sigmaE controls antioxidant defences required for *Salmonella virulence* and stationary-phase survival. *Mol. Microbiol.* **43**, 771–782 (2002).
74. S. C. Nang, M. A. K. Azad, T. Velkov, Q. T. Zhou, J. Li, Rescuing the last-line polymyxins: Achievements and challenges. *Pharmacol. Rev.* **73**, 679–728 (2021).
75. E. Massé, C. K. Vanderpool, S. Gottesman, Effect of RyhB small RNA on global iron use in Escherichia coli. *J. Bacteriol.* **187**, 6962–6971 (2005).
76. J. Hör, S. A. Gorski, J. Vogel, Bacterial RNA biology on a genome scale. *Mol. Cell* **70**, 785–799 (2018).
77. T. Møller, T. Franch, C. Udesen, K. Gerdes, P. Valentin-Hansen, Spot 42 RNA mediates discoordinate expression of the *E. coli* galactose operon. *Genes Dev.* **16**, 1696–1706 (2002).
78. E. Pasolli *et al.*, Extensive unexplored human microbiome diversity revealed by over 150,000 genomes from metagenomes spanning age, geography, and lifestyle. *Cell* **176**, 649–662.e20 (2019).
79. U. Schäfer, K. Beck, M. Müller, Skp, a molecular chaperone of gram-negative bacteria, is required for the formation of soluble periplasmic intermediates of outer membrane proteins. *J. Biol. Chem.* **274**, 24567–24574 (1999).
80. T. M. Kelly, S. A. Stachula, C. R. Raetz, M. S. Anderson, The firA gene of *Escherichia coli* encodes UDP-3-O-(R-3-hydroxymyristoyl)-glucosamine N-acyltransferase. The third step of endotoxin biosynthesis. *J. Biol. Chem.* **268**, 19866–19874 (1993).
81. A. Tsirigotaki, J. De Geyter, N. Šoštaric, A. Economou, S. Karamanou, Protein export through the bacterial Sec pathway. *Nat. Rev. Microbiol.* **15**, 21–36 (2017).
82. D. L. Leyton, A. E. Rossiter, I. R. Henderson, From self sufficiency to dependence: Mechanisms and factors important for autotransporter biogenesis. *Nat. Rev. Microbiol.* **10**, 213–225 (2012).
83. N. P. Walsh, B. M. Alba, B. Bose, C. A. Gross, R. T. Sauer, OMP peptide signals initiate the envelope-stress response by activating DegS protease via relief of inhibition mediated by its PDZ domain. *Cell* **113**, 61–71 (2003).
84. S. E. Ades, L. E. Connolly, B. M. Alba, C. A. Gross, The Escherichia coli sigma(E)-dependent extracytoplasmic stress response is controlled by the regulated proteolysis of an anti-sigma factor. *Genes Dev.* **13**, 2449–2461 (1999).
85. B. M. Alba, J. A. Leeds, C. Onufryk, C. Z. Lu, C. A. Gross, DegS and YaeL participate sequentially in the cleavage of RseA to activate the sigma(E)-dependent extracytoplasmic stress response. *Genes Dev.* **16**, 2156–2168 (2002).
86. R. Greenwell, T. W. Nam, T. J. Donohue, Features of Rhodobacter sphaeroides ChrR required for stimuli to promote the dissociation of σ(E)/ChrR complexes. *J. Mol. Biol.* **407**, 477–491 (2011).
87. J. Green, J. C. Crack, A. J. Thomson, N. E. LeBrun, Bacterial sensors of oxygen. *Curr. Opin. Microbiol.* **12**, 145–151 (2009).
88. H. Salvail, E. Massé, Regulating iron storage and metabolism with RNA: An overview of posttranscriptional controls of intracellular iron homeostasis. *Wiley Interdiscip. Rev. RNA* **3**, 26–36 (2012).
89. B. Troxell, H. M. Hassan, Transcriptional regulation by Ferric Uptake Regulator (Fur) in pathogenic bacteria. *Front. Cell. Infect. Microbiol.* **3**, 59 (2013).
90. E. Massé, S. Gottesman, A small RNA regulates the expression of genes involved in iron metabolism in Escherichia coli. *Proc. Natl. Acad. Sci. U.S.A.* **99**, 4620–4625 (2002).
91. B. M. Carpenter, J. M. Whitmire, D. S. Merrell, This is not your mother's repressor: The complex role of fur in pathogenesis. *Infect. Immun.* **77**, 2590–2601 (2009).
92. A. G. Oglesby-Sherrouse, E. R. Murphy, Iron-responsive bacterial small RNAs: Variations on a theme. *Metallomics* **5**, 276–286 (2013).
93. M. Mann, P. R. Wright, R. Backofen, IntaRNA 2.0: enhanced and customizable prediction of RNA–RNA interactions. *Nucleic Acids Research* **45**, W435–W439 (2017).
94. A. Manson McGuire *et al.*, Evolution of invasion in a diverse set of Fusobacterium species. *mBio* **5**, e01864 (2014).
95. C. Gur *et al.*, Binding of the Fap2 protein of *Fusobacterium nucleatum* to human inhibitory receptor TIGIT protects tumors from immune cell attack. *Immunity* **42**, 344–355 (2015).
96. J. Abed *et al.*, Fap2 mediates *Fusobacterium nucleatum* colorectal adenocarcinoma enrichment by binding to tumor-expressed Gal-GalNAc. *Cell Host Microbe* **20**, 215–225 (2016).
97. M. Olejniczak, X. Jiang, M. M. Basczok, G. Storz, KH domain proteins: Another family of bacterial RNA matchmakers? *Mol. Microbiol.* **117**, 10–19 (2021).
98. J. J. Zheng, A. J. Perez, H. T. Tsui, O. Massidda, M. E. Winkler, Absence of the KhpA and KhpB (JAG/EloR) RNA-binding proteins suppresses the requirement for PBP2b by overproduction of FtsA in Streptococcus pneumoniae D39. *Mol. Microbiol.* **106**, 793–814 (2017).
99. V. Lamm-Schmidt *et al.* Grad-seq identifies KhpB as a global RNA-binding protein in Clostridioides difficile that regulates toxin production. *microLife* **2**, uqab004 (2021).
100. K. J. Livak, T. D. Schmittgen, Analysis of relative gene expression data using real-time quantitative PCR and the 2(-Delta Delta C(T)) Method. *Methods* **25**, 402–408 (2001).
101. C. A. Schneider, W. S. Rasband, K. W. Eliceiri, NIH Image to ImageJ: 25 years of image analysis. *Nat. Methods* **9**, 671–675 (2012).
102. T. L. Bailey, J. Johnson, C. E. Grant, W. S. Noble, The MEME suite. *Nucleic Acids Res.* **43** (W1), W39–W49 (2015).
103. J. Vogel, Expanding the genetic toolkit helps dissect a global stress response in the early-branching species *Fusobacterium nucleatum*. NCBI Gene Expression Omnibus. https://www.ncbi.nlm.nih.gov/geo/query/acc.cgi?acc=GSE192339. Deposited 21 December 2021.
104. J. Vogel, Constitutive GFP-expression vector for *Fusobacterium nucleatum*. Addgene. https://www.addgene.org/187840/. Deposited15 August 2022.
105. J. Vogel, Constitutive mCherry-expression vector for Fusobacterium nucleatum. Addgene. https://www.addgene.org/187841/. Deposited 15 August 2022.
106. J. Vogel, Constitutive mScarlet-expression vector for Fusobacterium nucleatum. Addgene. https://www.addgene.org/187842/. Deposited 15 August 2022.
107. J. Vogel, Constitutive mNeonGreen-expression vector for *Fusobacterium nucleatum*. Addgene. https://www.addgene.org/187843/. Deposited 15 August 2022.
108. J. Vogel, Suicide vector to generate markerless gene deletions in *Fusobacterium nucleatum*. Addgene. https://www.addgene.org/187839/. Deposited 15 August 2022.
109. J. Vogel, Backbone for inducible expression system in Fusobacterium nucleatum. Addgene. https://www.addgene.org/187838/. Deposited 15 August 2022.
110. J. Vogel, Backbone for translational reporter system in Fusobacterium nucleatum. Addgene. https://www.addgene.org/187837/. Deposited 15 August 2022.
111. J. Vogel, Backbone for transcriptional reporter system in *Fusobacterium nucleatum*. Addgene. https://www.addgene.org/187836/. Deposited 15 August 2022.